IEEE Transactions on Circuits and Systems II, Vol. 43, pp. 207–219, Mar. 1996

A Closed Form Expression for an Efficient Class of Quadrature Mirror Filters and Its FIR Approximation *

Ajay Divakaran
William A. Pearlman
Electrical, Computer and Systems Engineering Department
Rensselaer Polytechnic Institute, Troy, NY 12180
e-mail: pearlman@ecse.rpi.edu
Phone: (518) 276-6082

Abstract

We find a simple closed form expression for an efficient class of Quadrature Mirror Filters (QMFs) by exploiting the inherent symmetry of the QMF property. We derive a simple rule of thumb to calculate the maximum feasible frequency selectivity of the filter for a given number N of filter taps. We show that, for even n, the frequency selectivity of a $2n+1$ or $2n$ tap filter can be increased if and only if the number of taps is increased by at least 4. Most existing QMFs closely match the derived analytical expression as well as verify the results on frequency selectivity. We obtain FIR implementations of the aforementioned analytical expression by using the Remez allocation algorithm. We choose weighting functions that confine the error to the intersection of the transition band and the stop band of the filter, as well as force the magnitude of the passband ripple to be much lower than that of the stopband ripple. We make such a choice in order to optimally satisfy the power complementarity condition as well as to attain high stop band attenuation. Our implementations match existing designs in performance.

1 Introduction and Statement of the Problem

Figure 1 shows a Quadrature Mirror Filter (QMF) [EG77] analysis/synthesis filter bank. Perfect reconstruction is achieved if the output $y(n)$ is a perfect replica of the input $x(n)$. The reconstruction is perfect if the discrete-time Fourier transforms $H_l(\omega)$ and $H_u(\omega)$ of the impulse responses h_l (lowpass) and h_u (highpass) satisfy the following conditions:

$$H_u(\omega) = e^{j\omega} H_l(\pi - \omega) \tag{1}$$

$$|H_l(\omega)|^2 + |H_l(\pi - \omega)|^2 = 1 \tag{2}$$

The mirror symmetry of the filters about $\omega = \frac{\pi}{2}$ illustrated in figure 2 is a direct consequence of the power complementarity condition (2). Note that the 3dB point of each filter's response is at $\omega = \frac{\pi}{2}$.

*This work was supported in part by the National Science Foundation under Grant No. NCR-9004758. The U.S. Government has certain rights in this material.

Vaidyanathan [Vai85] has shown that the only linear phase lowpass FIR transfer function that satisfies the power complementarity condition (2) is the trivial function $H(\omega) = cos(\frac{\omega}{2})$, which can be implemented with 2 taps. However, with a modest number of taps, the power complementarity condition can be very closely approximated by linear phase filter-pairs which satisfy the mirror property i.e. the symmetry about $\omega = \frac{\pi}{2}$ illustrated in Figure 2.

The aim of QMF design is, therefore, to design a linear phase FIR filter $H(\omega)$ that best approximates the power complementarity condition.

This problem has been tackled in the frequency domain and the time domain [Joh80, PZ84, SA91, JC84]. These approaches have relied on linear and non-linear optimization of the reconstruction fidelity by means of numerical search algorithms. As a result, none of the existing designs has yielded a simple and general analytic framework for QMFs. In this paper, we derive simple closed form expressions for an efficient class of QMFs, derive FIR approximations thereof, and compare to existing QMF designs.

2 Other Approaches to Perfect Reconstruction

Since no FIR symmetric filter satisfies power complementarity, other Perfect Reconstruction schemes have sacrificed either linear phase or power complementarity, and thus we divide them into two categories accordingly. The first category consists of schemes such those proposed by Smith and Barnwell [SI84, SI86] and Vaidyanathan et al [VH88] that use FIR filters that are not linear phase. The second category consists of schemes such as those reported in [ABMD90, VH88, VD89, NV89, VH90, VG89, RV91, ABMD90] that use FIR linear phase filters that give rise to a non-orthogonal wavelet expansion, because they do not satisfy power complementarity. Note that approximate power complementarity implies approximate orthonormality of the underlying wavelet basis.

It is not clear that the filters described above will necessarily outperform QMFs significantly. The reconstruction error of a typical QMF is low enough to be insignificant when the input is quantized, especially with quantized images [ASH87]. Hence, the possibly deleterious effects of the loss of orthogonality may outweigh the slim advantage that theoretical perfect reconstruction provides. To quote Vaidyanathan and Hoang [VH88]:

> "For the linear phase case, perhaps the most judicious and practical scheme would be to use any of the techniques proposed over the last decade ([EG77, Joh80, GN84, JC84] ...) which do not insist on theoretical perfect reconstruction. These techniques are such that aliasing and phase distortion are completely eliminated (in spite of multiplier quantization) and amplitude distortion is minimized in a systematic fashion [JC84, Joh80]. In applications where linearity of phase is important, these earlier techniques seem to be most promising."

3 An efficient class of QMFs

We derive a class of efficient QMFs which require the fewest taps for FIR implementation, for a given passband width (see Figure 3). We let

$$H_p(\omega) = |H_l(\omega)|^2 \tag{3}$$

Then we can write an expression for a generic $H_p(\omega)$, which has zero attenuation in the pass band and infinite attenuation in the stop band, bearing in mind that the ultimate aim is to design a low pass filter.

$$H_p(\omega) = \begin{cases} 1, & \text{if } |\omega| < \omega_p \\ \text{f}(\omega), & \text{if } \omega_p < |\omega| < \pi - \omega_p \\ 0, & \text{otherwise} \end{cases} \tag{4}$$

We need only $f(\omega)$ and ω_p to define $H_p(\omega)$. $f(\omega)$ has the same mirror symmetry as does $H_p(\omega)$.

Let us try to establish a procedure that directly yields a suitable $f(\omega)$ for the given ω_p. Since $H_p(\omega)$ is a low pass filter and should be as smooth as possible (to facilitate FIR implementation) we can place the following requirements on $f(\omega)$:

$$f^{'}(\omega_p) = f^{'}(\pi - \omega_p) = 0 \tag{5}$$

and

1. $f(\omega)$ is strictly monotonic decreasing.

2. $f^{'}(\omega)$ is strictly monotonic decreasing on $[\omega_p, \frac{\pi}{2}]$.

Consider a class of functions $F(W)$, $W \in [0,1]$, such that :

$$F(0) = 1 \tag{6}$$

$$F(1) = 0 \tag{7}$$

$$F(W) + F(1-W) = 1 \tag{8}$$

$$F^{'}(0) = F^{'}(1) = 0 \tag{9}$$

Let us place the following requirements on F(W):

1. $F(W)$ is strictly monotonic decreasing on $[0,1]$.

2. $F^{'}(W)$ is strictly monotonic decreasing on $[0, \frac{1}{2}]$

Then we can get a feasible $f(\omega)$ by suitably scaling and translating F(W) i.e.

$$f(\omega) = F\left(\frac{\omega - \omega_p}{\pi - 2\omega_p}\right) \tag{10}$$

3.1 How to generate F(W)

The preceding conditions on $F(W)$ do not give us an obvious way to generate a typical $F(W)$. Consider a typical $F(W)$ as shown in figure 4. Let us draw a typical $F^{'}(W)$. Condition 1 on the class $F(W)$ ensures that $F^{'}(W)$ is nonpositive $\forall\ W \in [0,1]$. Condition 2 on $F(W)$ ensures that $F^{'}(\frac{1}{2})$ is the minimum and (8) and (9) imply that $F^{'}(W)$ is even symmetric about $W = \frac{1}{2}$. In fact, all odd order derivatives of $F(W)$ are even symmetric about $W = \frac{1}{2}$, and all even order derivatives of $F(W)$ are odd symmetric or antisymmetric about $W = \frac{1}{2}$.

Let us differentiate $F^{'}(W)$ to look at a typical $F^{''}(W)$, as illustrated in figure 6. We can write down the following characteristics:

1. $F^{''}(W)$ is monotonic increasing on [0,1].

2. $F^{''}(W)$ is odd symmetric about $W = \frac{1}{2}$.

These conditions are quite easy to meet and we can thus generate a whole family of $F(W)$ by choosing $F^{''}(W)$ that satisfy the preceding requirements. To eliminate any kinks, which would adversely affect the FIR implementation, we impose convexity on $F^{''}(W)$. In other words,

3. $F^{''}(W)$ is convex $\cap$ or convex $\cup$ on $[0, \frac{1}{2}]$. We divide the $F(W)$ into two types.

Definition 1: Type 1 consists of F(W) such that $F^{''}(W)$ is convex $\cap$ on [0,$\frac{1}{2}$]. Type 2, on the other hand, consists of F(W) such that $F^{''}(W)$ is convex $\cup$ on [0,$\frac{1}{2}$].

We can thus generate a valid $F(W)$ in three steps:

Step 1 : Choose a function $P(W)$ which is monotonic increasing, odd symmetric about $W = \frac{1}{2}$, and convex $\cap$ or convex $\cup$ on [0,$\frac{1}{2}$].

Step 2 : $F^{'}(W)$ is given by,

$$F^{'}(W) = k\int_0^W P(T)\,dT \tag{11}$$

where k is a constant which we can compute in the final stage.

Proof : Let

$$Q(W) = k\int_0^W P(T)\,dT \tag{12}$$

Since $P(W)$ is odd symmetric about $W = \frac{1}{2}$ and monotonic increasing,

$$Q(0) = Q(1) = 0 \tag{13}$$

and $Q(W)$ is even symmetric about $W = \frac{1}{2}$ and $Q(W)$ has exactly one minimum at $W = \frac{1}{2}$. Finally, $Q(W)$ is nonpositive for all W $\in$ [0,1]. Hence, $Q(W)$ satisfies all the conditions for a valid $F^{'}(W)$.

Step 3 : $F(W)$ is given by,

$$F(W) = \frac{R(1) - R(W)}{R(1)} \tag{14}$$

where

$$R(W) = \int_0^W F^{'}(T)\,dT \tag{15}$$

Proof : Let

$$S(W) = \frac{R(1) - R(W)}{R(1)} \tag{16}$$

From the expression for $R(W)$ we get

$$R(0) = 0 \tag{17}$$

and $R(1)$ is the minimum $\forall W \in [0,1]$, and

$$R(1) = -p \tag{18}$$

where p is a positive number because $R(W)$ is nonpositive $\forall$ $W \in$ [0,1]. Then

$$S(1) = \frac{R(1) - R(1)}{R(1)} = 0 \tag{19}$$

and

$$S(0) = \frac{R(1) - R(0)}{R(1)} = \frac{-p - 0}{-p} = 1 \tag{20}$$

and $S(\frac{1}{2}) = \frac{1}{2}$ because of the even symmetry of $F^{'}(W)$ about $W = \frac{1}{2}$. The even symmetry of $F^{'}(W)$ about $W = \frac{1}{2}$ also causes $S(W)$ to be mirror symmetric about $W = \frac{1}{2}$. $S(W)$ is clearly monotone decreasing on [0,1]. Hence, $S(W)$ meets all the requirements for a valid $F(W)$.

3.2 The two extremes of $F(W)$

We can generate a whole family of $F(W)$ by choosing

$$P(W) = (W - \frac{1}{2})^{2n+1}$$

These functions are convex $\cup$ on $[\frac{1}{2}, 1]$, and satisfy all the requirements mentioned earlier. As we increase n, the $F(W)$ begin to resemble $F_{stline}(W) = 1 - W$. In fact, with $n = 12$ (i.e.$P(W) = (W - \frac{1}{2})^{25}$) we find that:

$$F(W) \approx 1 - W.$$

This indicates that as n becomes arbitrarily large, $F(W)$ becomes a straight line, and hence the corresponding filter tends to become a *straight line transition band* filter. The straight line transition band filter therefore does represent one extreme, even though it is not C^1 continuous and hence does not satisfy the requirements on $F(W)$ that we imposed earlier. With this in mind, we will from now on refer to it as one of the extremes.

The other extreme is $F(W)$ such that $F''(W)$ is the signum function centered at $W = \frac{1}{2}$. In contrast with the straight line transition band filter, this extreme has better continuity at 0 and 1 but there is a step discontinuity in the second derivative at $W = \frac{1}{2}$. We will refer to this extreme as the *signum filter*. The $F(W)$ for this transition band shape is given by:

$$F(W) = \begin{cases} 1 - 2W^2, & \text{if } W \in [0, \frac{1}{2}] \\ 2(1 - W)^2, & \text{if } W \in [\frac{1}{2}, 1] \end{cases} \tag{21}$$

Now that we have a simple procedure to generate $F(W)$ and thus $f(\omega)$ for a given ω_p, we need to choose a good $P(W)$. Intuitively we would expect that an $F(W)$ that is very steep at $W = \frac{1}{2}$ (recall that the signum filter's second derivative has infinite slope at $\omega = \frac{\pi}{2}$) will not yield an easy to implement FIR filter. On the other hand, an $F(W)$ that is not too steep at $W = \frac{1}{2}$ could have an abrupt transition around $W = 1$ and $W = 0$, which would cause implementation problems. We illustrate these two extremes in Figures 8 and 9. Note that the two extremes belong to two distinct categories, Type 1 and Type 2 as defined earlier. Note that $P(W) = W - \frac{1}{2}$ falls in both categories and should therefore be a good starting function in our search for an $F(W)$ that behaves well at $W = \frac{1}{2}$ as well as around the end points of $[0, 1]$.

3.3 What is the best $f(\omega)$?

Any linear phase FIR implementation of these filters will be an approximation of the ideal impulse response. For a given passband edge frequency ω_p and permissible approximation error, the product filter with the fastest converging Fourier series will require the fewest taps and will thus yield a QMF which in turn requires the fewest taps.

Hence it is sufficient to find an $H_p(\omega)$ with a fast converging impulse response $h_p(n)$ in order to obtain an easy to implement QMF.

3.4 The optimal $f(\omega)$

We can show that $f(\omega)$ such that

$$f''''(\omega) = 0 \tag{22}$$

yields an $H_p(\omega)$ which requires the fewest taps for FIR implementation, for a given maximum permissible mean square difference between the ideal definition (4) and its FIR approximation. This follows from an analysis of the rate of the convergence of the Fourier series of $H_p(\omega)$. Equation (3) implies that the corresponding QMF $H_l(\omega)$ will also require the fewest taps for FIR implementation.

3.4.1 Proof

Using the mirror symmetry of $H_p(\omega)$, we have derived in the appendix the Fourier series expansion as follows:

$$H_p(\omega) = \frac{1}{2} + \sum_{n=1}^{\infty} T(n) cos(n\omega) \tag{23}$$

$$T(n) = 0 \tag{24}$$

for even n and

$$\begin{aligned} T(n) = -\frac{2}{\pi}\left[\frac{2f''(\pi-\omega_p)sin(n\omega_p)}{n^3}\right] \\ +\frac{2}{\pi}\left[\frac{f'''(\omega_p)cos(n\omega_p)}{n^4}\right] \\ +\frac{2}{\pi}\left[\int_{\omega_p}^{\pi-\omega_p} f''''(\omega)\frac{cos(n\omega)}{n^4}\, d\omega\right] \end{aligned} \tag{25}$$

for odd n.

Let $f_0(\omega)$ be a feasible $f(\omega)$ such that:

$$f_0''''(\omega) = 0 \tag{26}$$

Let us look at a feasible $f(\omega)$ which lies very close to $f_0(\omega)$,

i.e.$f(\omega)$ such that

$$f''''(\omega) \approx 0$$

These $f(\omega)$ correspond to $F(W)$ of Type 1 and Type 2 as per Definition 1 (see section 3.1). The corresponding properties are:

Type 1: $f''''(\omega)$ is monotonic increasing on $[\omega_p, \pi-\omega_p]$.

Type 2: $f''''(\omega)$ is monotonic decreasing on $[\omega_p, \pi-\omega_p]$.

We illustrate this in figure 10, and the corresponding $f'''(\omega)$ in figure 11.

For the aforementioned class of $f(\omega)$, the Fourier series expansion (23, 24) implies that, for non-trivial ω_p, it is the first term of order $O(n^{-3})$ that determines how fast the expansion converges.

Hence for this class of $f(\omega)$, for small changes in $f''''(\omega)$, we need only to study the change in $f''(\pi-\omega_p)$.

Let us study the variation in $f''(\pi-\omega_p)$ as we make small changes in $f_0(\omega)$. Let us change $f_0(\omega)$ slightly so that it becomes a Type 2 $f(\omega)$. We can easily plot the corresponding changes in $f''''(\omega)$ and $f'''(\omega)$ (see figure 12). Since $f_0''''(\omega) = 0$, $f_0'''(\omega) = c$ where c is a constant. For small shifts in $f''''(\omega)$ the $\cup$ convexity of $f''(\omega)$ implies that

$$f'''(\frac{\pi}{2}) < f'''(\pi-\omega_p) = f'''(\omega_p)$$

Let the shaded areas be A_1 and A_2. Then the change in $f''(\pi-\omega_p)$ is:

$$\Delta f''(\pi-\omega_p) = A_1 - A_2 \tag{27}$$

where

$$\Delta f''(\pi-\omega_p) = f''(\pi-\omega_p) - f_0''(\pi-\omega_p) \tag{28}$$

Since $f_0^{'''}(\omega) = c$, for very small $f^{''''}(\omega)$ i.e. $f(\omega)$ such that $f^{''''}(\omega) \approx 0$,

$$A_1 = A_2 \tag{29}$$

This follows from the $\cap$ convexity of $f^{''}(\omega)$ which causes the mirror symmetry of $f^{'''}(\omega)$ about the straight line $f(\omega) = c$. Therefore, there is no change in $f^{''}(\pi - \omega_p)$ i.e.

$$\Delta f^{''}(\pi - \omega_p) = 0 \tag{30}$$

Analogous arguments give the same result when we change $f_0(\omega)$ to a $f(\omega)$ of Type 1.

Since $f^{''}(\pi - \omega_p)$ remains constant when we make very small changes in $f_0(\omega)$ to make it a Type 1 or Type 2 $f(\omega)$, the rate of convergence of the Fourier expansion also remains constant. This means that $f_0(\omega)$ represents a local minimum because both extremes of $f(\omega)$ have slowly converging Fourier expansions. The first term of the Fourier expansion exclusively determines the rate of convergence only if $f^{''}(\pi - \omega_p)$ is non-negligible. Negligible $f^{''}(\pi - \omega_p)$ implies a higher effective ω_p and hence implies a slower Fourier expansion convergence. For moderate to high $f^{''}(\pi - \omega_p)$. the area cancellation takes place if and only if $f^{'''}(\omega) = constant$. Hence, $f_0(\omega)$ being the only local optimum is also the global optimum. An important consequence of this choice of $f(\omega)$ is that the shape of $f(\omega)$ is independent of the value of ω_p

Let us clarify this result by considering the two extremes viz. the signum filter and the straight line transition band filter (see Figures 8 and 9). The signum filter has zero $f^{''}(\pi - \omega_p)$, but has a high slope at $\omega = \frac{\pi}{2}$. This high slope causes very slow convergence of the Fourier expansion. To make the convergence faster, we need to reduce the slope at $\omega = \frac{\pi}{2}$. As we reduce the slope, $f^{''}(\pi - \omega_p)$ begins to increase. At first, this increase is very slow. This implies that as long as the slope at $\omega = \frac{\pi}{2}$ is high, $f^{''}(\pi - \omega_p)$ has little influence on the rate of convergence. All the gain in the rate of convergence is got by reducing the slope at $\omega = \frac{\pi}{2}$. Since a slight increase in $f^{''}(\pi - \omega_p)$ actually speeds up the convergence at this extreme, increasing $f^{''}(\pi - \omega_p)$ is actually beneficial.

Let us look at the other extreme, viz. the straight line transition band filter. The slope at $\omega = \frac{\pi}{2}$ is not very high but the $f^{''}(\pi - \omega_p)$ is arbitrarily large. The abrupt change of slope at $\omega = \omega_p$ introduces higher order terms in the Fourier series expansion. The slope at $\omega = \frac{\pi}{2}$ has much less influence on the rate of convergence than the value of $f^{''}(\pi - \omega_p)$. If we reduce $f^{''}(\pi - \omega_p)$ slightly, we get a gain in the rate of convergence because the slope at $\omega = \frac{\pi}{2}$ does not become significantly steeper. So, from this extreme, decreasing $f^{''}(\pi - \omega_p)$ is beneficial.

It is clear now that we need to reconcile two conflicting requirements:

1. The slope at $\omega = \frac{\pi}{2}$ should not be too high.

2. The value of $f^{''}(\pi - \omega_p)$ should not be too high.

Hence, the best $f(\omega)$ definitely lies in the middle, where $f^{''}(\pi - \omega_p)$ is of moderate magnitude. We have shown that for such $f(\omega)$, $f_0(\omega)$ is the best choice. *We can also now see why this represents a maximum for rate of convergence and not a minimum.*

3.5 The efficient class of QMFs

Recall that we need only $f(\omega)$ and ω_p to completely define the product filter $H_p(\omega)$. Now that we have established that the shape of $f(\omega)$ is the same for all ω_p, we can get a very simple expression for $H_p(\omega)$ which has only one variable parameter viz. ω_p.

Let $f(\omega) = f_0(\omega)$ and let the corresponding $F(W)$ be $F_{opt}(W)$. Then, since $f''''(\omega) = f_0''''(\omega) = 0$,

$$F_{opt}''''(W) = 0 \tag{31}$$

which implies that $F_{opt}''(W)$ is a first order polynomial in W i.e. $F_{opt}''(W)$ can be represented by a straight line. The requirements on the class of functions $F(W)$ imply that

$$F_{opt}''(W) = k(W - \frac{1}{2}) \tag{32}$$

where k is a constant. This corresponds to choosing

$$P(W) = W - \frac{1}{2} \tag{33}$$

in the three step process described in section 2.1. Carrying out the three step process we obtain,

$$F_{opt}(W) = 2W^3 - 3W^2 + 1 \tag{34}$$

Let the aforementioned choice of $f(\omega)$ be $f_{opt}(\omega)$. Then, using equation (10) we get:

$$f_{opt}(\omega) = (1 - W)^2(2W + 1) = 2W^3 - 3W^2 + 1 \tag{35}$$

where the value of W is given by,

$$W = \frac{\omega - \omega_p}{\pi - 2\omega_p}, \tag{36}$$

and hence,

$$\sqrt{f_{opt}(\omega)} = (1 - W)\sqrt{(2W + 1)}. \tag{37}$$

The efficient class of QMFs $H_{eff}(\omega)$ is given by,

$$H_{eff}(\omega) = \begin{cases} 1, & \text{if } |\omega| < \omega_p \\ \sqrt{f_{opt}(\omega)}, & \text{if } \omega_p < |\omega| < \pi - \omega_p \\ 0, & \text{otherwise} \end{cases} \tag{38}$$

The impulse response $H_{eff}(z)$ is given by,

$$H_{eff}(z) = \sum_{-\infty}^{\infty} h_{eff}(n) z^{-n}, \tag{39}$$

$$h_{eff}(n) = \frac{1}{2\pi}\int_{-\pi}^{\pi} H_{eff}(\omega) cos(n\omega)\, d\omega. \tag{40}$$

The function $\sqrt{f_{opt}(\omega)}$ can easily be expanded in a Taylor series in ω about $\omega = \frac{\pi}{2}$. In practice, five Taylor series terms should suffice for a good approximation. We can then get approximate closed form expressions for the impulse response $h_{eff}(n)$ as well.

4 Comparison with existing designs: Analytical and Numerical results

We derive a simple rule of thumb to calculate the maximum feasible ω_p for a given number N of filter taps, denoted by $\omega_{p,max}(N)$.

To find out how well we can do with $N = 2n + 1$ taps, we need to look at the Fourier coefficients ($h_{eff}(k)$) of order $k > n$. This is because a $2n + 1$ tap FIR approximation is essentially a truncation of the Fourier series after the n^{th} term, e.g., a 9 tap filter is equivalent to a truncation after the 4^{th} term $(0, \pm1, \pm2, \pm3, \pm4)$. Such a truncation will yield a good approximation only if the higher order Fourier coefficients are negligible. We restrict our attention to the first two of the Fourier coefficients of order $k > n$. We plot just the $(n+1)^{th}$ and $(n+2)^{th}$ Fourier coefficients ($h_{eff}(n)$) versus the passband width ω_p. It is reasonable to assume that as long as these two coefficients are negligibly low in magnitude, the $N = 2n + 1$ tap FIR approximation will be accurate, given of course that the coefficients of order $k > n + 2$ are also negligible. As ω_p increases, these coefficients assume more and more significance because the frequency selectivity of the filter goes up. The increase in the magnitude of these coefficients is not monotonic but tends to go through a series of maxima and minima. We illustrate this in figure 11 in which we plot the fifth and sixth coefficients versus the passband width ω_p, to see how we do with 9 taps. For values of $\omega_p$that lie between the intersections of these plots with the ω_p axis, the magnitudes of these coefficients are negligible. At such values, the FIR approximation will hence be accurate, if the magnitudes of the coefficients of order $k > 6$ are also negligible. This implies that the maximum feasible passband edge frequency $\omega_{p,max}(N)$ lies between one of the closely spaced pairs of intersections of the plots with the ω_p axis (See figure 11). Thus we only need to choose the pair of intersections which gives the highest value for the $\omega_{p,max}(N)$. In this case $N = 9$. As shown, we reject the first intersection pair because we get a value of $\omega_{p,max}(9)$ that is less than what we could get with just five taps. The second pair of intersections gives a value that improves upon the passband width of the five tap filter. We stop at this pair because subsequent intersections are at values of ω_p which are so high that the coefficients of order greater than 6 cease to be negligible. This turns out to be a recurring pattern. We can thus generalize this procedure for $N = 2n+1$ taps and say that the maximum feasible passband edge frequency $\omega_{p,max}(N)$ will lie between the first non-trivial intersection of the amplitude of the $(n+1)^{th}$ coefficient with the ω_p axis and that of the $(n+2)^{th}$ coefficient with the $\omega_p$axis. We define a *non-trivial intersection* as an intersection ω_{int} such that ω_{int} is greater than the maximum feasible passband edge frequency for $N - 2$ taps. i.e.

$$\omega_{int} \geq \omega_{p,max}(N-2)$$

In this region, both coefficients have a suitably low magnitude. Only the first non-trivial intersections will yield correct values of $\omega_{p,max}(N)$ because the magnitude of the higher order coefficients will not be negligible at subsequent intersections. An analogous formulation reaches the same conclusions for an even number of taps, where $N = 2n$.

The preceding arguments allow us to state our Rule of Thumb:

Rule of Thumb : The maximum feasible passband edge frequency $\omega_{p,max}(N)$ lies between the first non-trivial intersections of the $(n+1)^{th}$ and the $(n+2)^{th}$ coefficients with the ω_p axis, and can be estimated from the plots, where $N = 2n + 1$ or $N = 2n$.

We illustrate the application of this rule of thumb in figure 11 in which we plot the fifth and sixth coefficients to calculate $\omega_{p,max}(9)$. Note that we choose the intersection of the two plots in the region of interest as the estimated value.

Application of the rule of thumb shows that the convenient positioning of the intersections illustrated in figure 11 occurs only for every other pair $n + 1$ and $n + 2$ of coefficients. This is because the even and odd coefficient intersections with the ω_p axis are "staggered" in such a way that only every other pair of consecutive coefficients has conveniently located intersections with the ω_p axis. For instance, the intersections of the fourth and fifth coefficients are spaced so wide apart that the higher order coefficients are no longer negligible at the estimated $\omega_{p,max}(N)$ got from the rule of thumb. At the intersection of the fourth coefficient and the $\omega_p$axis, the fifth coefficient is not negligible. Hence, the $\omega_{p,max}(N)$ is unchanged, i.e. the seven tap filter is not able to improve upon the frequency selectivity of the five tap filter in spite of the increased taps. An analogous argument holds for even tap implementation. We can sum up this result as follows:

$$\omega_{p,max}(2n+1) = \omega_{p,max}(2n+3) \tag{41}$$

$$\omega_{p,max}(2n) = \omega_{p,max}(2n+2) \tag{42}$$

for even n.

Equations (41) and (42) imply that for even n, the frequency selectivity of a $2n+1$ or $2n$ tap filter can be improved if and only if the number of taps is increased by at least 4. Existing designs[SA91, Sim88] verify these results. It is interesting to note that Pirani and Zingarelli [PZ84] and Johnston [Joh80] present even tap designs in increments of at least four taps in the manner predicted by our result, but do not give any reason for doing so.

One reason our simple strategy of considering the first two higher order coefficients succeeds so well is that the function $H_{eff}(\omega)$ is "well behaved," so that when ω_p increases, it is these two coefficients that first assume significance. For instance, the fifth higher order coefficient does not suddenly assume significance much before the second higher order coefficient does. If the function $H_{eff}(\omega)$ were not "nice," the conveniently placed intersections depicted in Figure 13 would not help, because the first two higher order coefficients would no longer play a consistent role in the FIR approximation.

It is important to note that our rule of thumb yields ω_p such that the best compromise is achieved between adherence to power complementarity and frequency selectivity. Hence equations (41) and (42) imply only that the ω_p that achieves the best compromise is unchanged even if we increase the number of taps by two. They **do not** imply that the adherence to power complementarity, i.e. the reconstruction fidelity, is also unchanged. For the same value of ω_p, increasing the taps by two will always improve the reconstruction fidelity.

Most existing QMFs closely match the analytical expression derived here when we substitute ω_p = effective $\omega_p \approx \omega_{p,max}(N)$, where $\omega_{p,max}(N)$ is obtained, in radians, as described earlier and N is the number of taps. Recall that the ω_p is the only variable parameter in the analytical expression. We illustrate this in figure 14 in which we compare Johnston's [Joh80] 32 tap C filter with the analytical expression, with $\omega_p = 1.32 \approx \omega_{p,max}(32) = 1.31$.

5 Implementation (FIR Approximation)

Since there is no non-trivial FIR filter that exactly satisfies the power complementarity condition, what we mean by "implementation" in this section, is in fact FIR approximation. Rectangular window implementations of the filters yield filters which are only marginally inferior to existing designs. We illustrate this in Figure 15. Note that the 32 tap rectangular window implementation has sharper cut-off (steeper roll-off) but has more ripple than Johnston's 32 tap C filter. The rectangular window technique is simple but it is highly susceptible to the Gibbs phenomenon i.e. it causes excessive ringing. Since we do have closed form expressions for the frequency response, we can use more sophisticated FIR implementation techniques like advanced windowing techniques or the Remez allocation algorithm [RG75].

The power complementarity condition indicates that passband ripple is much less tolerable than stopband ripple, because any passband ripple in $|H(\omega)|$ is aggravated in $|H(\omega)|^2$ while the stopband ripple actually reduces. We illustrate this in figure 16. Stopband ripple, though relatively tolerable, is still undesirable because it adversely affects the frequency selectivity of the filter. The best strategy is therefore to let the region about the intersection of the transition band and the stop band absorb most of the error. In fact, existing QMFs also seem to end up confining the bulk of the error to this region. See, for instance , the illustration of Johnston's 32 tap C filter.

We try some weighting functions shaped accordingly, i.e. we place heavy weights on the passband and relatively light weights in the stop band, and implement the filters using the Remez allocation algorithm. We use the 'remez' function of the Matlab package. Our input consists of a grid of the desired frequency response and a weight vector. The grid is finer in the transition band, while the passband and the stop band are just described in terms of their edges. This is because it is the transition band that is crucial to the maintenance of the power complementarity. We apply very light weights to the values around the intersection of the transition band and the stop band. This ensures a smooth transition devoid of Gibbs ringing. Furthermore, it turns out that we need to weight the response at $\omega = \frac{\pi}{2}$ very heavily to get the best adherence to the power complementarity. We have implemented 32, 16 and 9 tap filters respectively. We present the frequency response of the nine tap design at the end of this section. Our nine tap filter equals the nine tap filter of Simoncelli[ASH87]. We illustrate this in Figures 17 and 18. Note that the frequency responses of the two filters are practically indistinguishable. It is only in the logarithmic domain that some differences can be seen. We compare the allpass characteristic of Simoncelli's 9 tap filter with that of our 9 tap filter in Figure 19. We carry out a two dimensional separable subband decomposition and synthesis with our 9 tap filter on some common 256x256 images and get consistently better reconstruction fidelity than does Simoncelli's filter. We compare reconstruction errors obtained from our 9 tap design with those obtained from Simoncelli's design in Table 2. Note that the reconstruction fidelity suffers as the number of stages in the pyramid is increased, but with three stages, the SNR is still very high (65 dB at least). Our 16 and 32 tap implementations are only slightly inferior to existing designs. This is because we have chosen a relatively sparse input grid.

Finally, we compare the square of the filter characteristics with the square of the analytical expression with an appropriately substituted value of the passband edge frequency ω_p. Note that (see Figures 20, 21 and 22) the FIR filter characteristic rounds or chamfers the sharp corners of the analytical expression at the edges of the transition band, but there is an excellent match elsewhere.

The main purpose of these implementations is to show that our formula for the efficient class of filters does in fact yield good filters in practice. Note that the weighting strategy makes the choice of $f(\omega)$ almost irrelevant, since all $f(\omega)$ that satisfy power complementarity have the same value viz. $\frac{1}{2}$, at $\omega = \frac{\pi}{2}$ which is the only transition band value that is weighted heavily i.e. ensured. However, the final FIR approximations have frequency responses that closely match the analytical formula. For instance, if $f(\omega)$ is chosen to be a straight line from ω_p to $\pi - \omega_p$, there is a high mismatch between the formula and the practical filter characteristic. If we use a shape different from our "efficient" formula for $f(\omega)$, the precision of the results from the rule of thumb goes down. The intersections will be wider spaced and hence will give a wider range for feasible maximum ω_p. Furthermore, we will not have a general analytical framework for QMFs on account of the severe mismatch mentioned earlier. In subsequent work, we have made use of the analytical formula to derive useful results on information theoretic performance as well as on the associated wavelet basis [Div93],[DP95].

As mentioned earlier, our nine tap filter equals the nine tap filter of Simoncelli's filter in performance. We can also equal other higher order implementations (such as 16 and 32 tap), by using finer grids. Our approach offers some advantages viz.

- Flexibility.

  Our approach, unlike other approaches, allows modification of the design. Modification of the design might be required in some cases e.g. when we can tolerate relatively low reconstruction fidelity but need to minimize computational expense and need to maximize frequency selectivity.

- Ease of implementation.

  We have used a widely available software package (Matlab). With the grid sizes that we used, i.e. ten samples in the transition band, the computational time is low.

- Better Insight.

  Since we work with a simple analytical formula and with a set of simple rules, we are able to get a better insight into the design. This in turn provides the flexibility we mentioned earlier.

We present the tap values for 9, 16 and 32 tap filters in Table 1.

6 Recapitulation

Let us sum up this paper. We reviewed QMF design techniques and found that none of the existing designs has yielded a simple and general analytical framework. We briefly looked at other perfect reconstruction techniques in order to motivate the study of power complementary QMFs. We derived a class of efficient QMFs which require the fewest taps for FIR implementation, for a given passband width. We did so by exploiting the inherent symmetry of the QMF property. We derived a simple rule of thumb to calculate the maximum feasible frequency selectivity of the filter for a given number N of filter taps. We showed that, for even n, the frequency selectivity of a $2n+1$ or $2n$ tap filter can be increased if and only if the number of taps is increased by at least 4. Most existing QMFs closely match the derived analytical expression as well as verify the results on frequency selectivity. We developed a new Remez allocation based algorithm for FIR implementation of the efficient class. Our implementations match existing designs in performance.

7 Acknowledgement

We would like to thank our reviewers for their valuable comments and suggestions.

8 Appendix

8.1 Fourier Series of $H_p(\omega)$

Though the expressions for the frequency responses are different, the even continuation expansion will converge fast if and only if the odd continuation half range expansion converges fast. Therefore, we can restrict our attention to the even continuation expansion without any loss of generality.

Recall the definition of $H_p(\omega)$:

$$H_p(\omega) = \begin{cases} 1 & \text{if } |\omega| < \omega_p \\ \mathrm{f}(\omega) & \text{if } \omega_p < |\omega| < \pi - \omega_p \\ 0 & \text{otherwise} \end{cases} \tag{43}$$

Let us write down the implications of the symmetry of $H_p(\omega)$ (see Figure 3).

1. The even symmetry about $\omega = 0$ implies that we have a cosine series.

2. The mirror symmetry about $\omega = \frac{\pi}{2}$ implies that the zero frequency term $T_0 = \frac{1}{2}$ and thus we can write:
$$H_p(\omega) = \frac{1}{2} + \sum_{n=1}^{\infty} T(n) cos(n\omega) \tag{44}$$

3. The mirror symmetry about $\omega = \frac{\pi}{2}$ implies that the even coefficients $T(n = 2 * k)$ will be zero. Hence, in the analysis that follows, we will assume odd n.

Now we are ready to calculate $T(n)$.
$$T(n) = \frac{2}{\pi}\int_0^{\pi} H_p(\omega) cos(n\omega)\, d\omega \tag{45}$$
or
$$T(n) = \frac{2}{\pi}\left[\int_0^{\omega_p} cos(n\omega)\, d\omega + \int_{\omega_p}^{\pi-\omega_p} f(\omega) cos(n\omega)\, d\omega\right] \tag{46}$$
Integrating by parts we get:
$$T(n) = \frac{2}{\pi}\left[\frac{sin(n\omega_p)}{n} + \left[\frac{f(\omega) sin(n\omega)}{n}\right]_{\omega_p}^{\pi-\omega_p} - \int_{\omega_p}^{\pi-\omega_p} f'(\omega)\frac{sin(n\omega)}{n}\, d\omega\right] \tag{47}$$
By definition $f(\omega_p) = 1$ and $f(\pi - \omega_p) = 0$ and hence:
$$T(n) = \frac{2}{\pi}\left[\frac{sin(n\omega_p)}{n} - \frac{sin(n\omega_p)}{n} - \int_{\omega_p}^{\pi-\omega_p} f'(\omega)\frac{sin(n\omega)}{n}\, d\omega\right] \tag{48}$$
Or
$$T(n) = \frac{2}{\pi}\left[-\int_{\omega_p}^{\pi-\omega_p} f'(\omega)\frac{sin(n\omega)}{n}\, d\omega\right] \tag{49}$$
On integrating this expression by parts we get:
$$T(n) = \frac{2}{\pi}\left[\left[\frac{f'(\omega) cos(n\omega)}{n^2}\right]_{\omega_p}^{\pi-\omega_p} - \int_{\omega_p}^{\pi-\omega_p} f''(\omega)\frac{cos(n\omega)}{n^2}\, d\omega\right] \tag{50}$$
Since by definition $f'(\omega_p) = f'(\pi - \omega_p) = 0$
$$T(n) = \frac{2}{\pi}\int_{\omega_p}^{\pi-\omega_p} -f''(\omega)\frac{cos(n\omega)}{n^2}\, d\omega \tag{51}$$
Integrating by parts we get:
$$T(n) = -\frac{2}{\pi}\left[\left[\frac{f''(\omega) sin(n\omega)}{n^3}\right]_{\omega_p}^{\pi-\omega_p} - \int_{\omega_p}^{\pi-\omega_p} f'''(\omega)\frac{sin(n\omega)}{n^3}\, d\omega\right] \tag{52}$$
We have pointed out in the previous section that all the even order derivatives of $f(\omega)$ are odd symmetric about $\omega = \frac{\pi}{2}$ and all the odd order derivatives are even symmetric about $\omega = \frac{\pi}{2}$. This implies that:
$$f''(\omega_p) = -f''(\pi - \omega_p)$$

Also, since $f^{''}(\omega)$ is monotonic increasing and odd symmetric about $\omega = \frac{\pi}{2}$,

$$f^{''}(\pi - \omega_p) \geq 0$$

and since n is odd,

$$sin(n\pi - n\omega_p) = sin(n\omega_p)$$

We can thus simplify the previous expression to get:

$$T(n) = -\frac{2}{\pi}\left[\frac{2f^{''}(\pi-\omega_p)sin(n\omega_p)}{n^3} - \int_{\omega_p}^{\pi-\omega_p} f^{'''}(\omega)\frac{sin(n\omega)}{n^3}\, d\omega\right] \tag{53}$$

Integrating by parts, we get:

$$T(n) = -\frac{2}{\pi}\left[\frac{2f^{''}(\pi-\omega_p)sin(n\omega_p)}{n^3} - \left[-\frac{f^{'''}(\omega)cos(n\omega)}{n^4}\right]_{\omega_p}^{\pi-\omega_p}\right]$$
$$-\frac{2}{\pi}\left[-\int_{\omega_p}^{\pi-\omega_p} f^{''''}(\omega)\frac{cos(n\omega)}{n^4}\, d\omega\right] \tag{54}$$

The even symmetry of $f^{'''}(\omega)$ about $\omega = \frac{\pi}{2}$ implies that

$$f^{'''}(\omega_p) = f^{'''}(\pi - \omega_p)$$

and since n is odd

$$cos(n\pi - n\omega_p) = -cos(n\omega_p)$$

We can thus simplify to get:

$$T(n) = -\frac{2}{\pi}\left[\frac{2f^{''}(\pi-\omega_p)sin(n\omega_p)}{n^3} - \frac{2f^{'''}(\omega_p)cos(n\omega_p)}{n^4} - \int_{\omega_p}^{\pi-\omega_p} f^{''''}(\omega)\frac{cos(n\omega)}{n^4}\, d\omega\right] \tag{55}$$

In short, the Fourier series expansion of $H_p(\omega)$ is :

$$H_p(\omega) = \frac{1}{2} + \sum_{n=1}^{\infty} T(n)cos(n\omega) \tag{56}$$

where $T(n)$ is given by:

$$T(n) = 0 \tag{57}$$

for even n and

$$T(n) = -\frac{2}{\pi}\left[\frac{2f^{''}(\pi-\omega_p)sin(n\omega_p)}{n^3} - \frac{2f^{'''}(\omega_p)cos(n\omega_p)}{n^4} - \int_{\omega_p}^{\pi-\omega_p} f^{''''}(\omega)\frac{cos(n\omega)}{n^4}\, d\omega\right] \tag{58}$$

for odd n.

REFERENCES

[ABMD90] M. Antonini, M. Barlaud, P. Mathieu, and I. Daubechies. Image coding using vector quantization in the wavelet transform domain. In *Proceedings ICASSP*, pages pp. 2297–2300, Albuquerque, NM, April 1990.

[ASH87] Edward H. Adelson, Eero Simoncelli, and Rajesh Hingorani. Orthogonal pyramid transforms for image coding. In *Proceedings of SPIE*, pages pp. 50–58, Cambridge, MA, October 1987.

[Div93] Ajay Divakaran. *Quadrature Mirror Filters: FIR Implementation, Wavelet Analysis and Information Theoretic Analysis*. PhD thesis, Department of Electrical, Computer, and Systems Engineering, Rensselaer Polytechnic Institute, August 1993.

[EG77] D. Esteban and C. Galand. Application of quadrature mirror filters to split band voice coding schemes. In *Proceedings ICASSP*, pages pp. 191–195, 1977.

[GN84] Claude R. Galand and Henri J. Nussbaumer. New quadrature mirror filter structures. *IEEE Transactions ASSP*, ASSP-32(3):pp. 522–531, June 1984.

[JC84] Vijay K. Jain and Ronald E. Crochiere. Quadrature mirror filter design in the time domain. *IEEE Transactions ASSP*, ASSP-32(2):pp. 353–360, April 1984.

[Joh80] J. D. Johnston. A filter family designed for use in quadrature mirror filter banks. In *Proceedings of the IEEE International Conference on Acoustics, Speech and Signal Processing (ICASSP)*, pages pp. 291–294, Denver, CO, April 1980.

[NV89] T. Q. Nguyen and P. P. Vaidyanathan. Two-channel perfect-reconstruction FIR QMF structures which yield linear-phase analysis and synthesis filters. *IEEE Transactions ASSP*, ASSP-37-5:pp. 676–690, May 1989.

[PZ84] Giancarlo Pirani and Valerio Zingarelli. An analytical formula for the design of quadrature mirror filters. *IEEE Transactions ASSP*, ASSP-32-3:pp. 645–648, June 1984.

[RG75] Lawrence R. Rabiner and Bernard Gold. *Theory and Application of Digital Signal Processing*. Prentice-Hall, Englewood Cliffs, NJ, 1975.

[RV91] Olivier Rioul and Martin Vetterli. Wavelets and signal processing. *IEEE Signal Processing Magazine*, vol. 8, no. 4:pp. 14–38, October 1991.

[SA91] Eero P. Simoncelli and Edward H. Adelson. Subband transforms. In John W. Woods, editor, *Subband Image Coding*, pages Chapter 4, pp. 143–192. Kluwer Academic Publishers, 1991.

[SI84] M. J. T. Smith and T. P. Barnwell III. A procedure for designing exact reconstruction filter banks for tree-structured subband coders. In *Proceedings ICASSP*, pages pp. 27.1–27.1.4, 1984.

[SI86] Mark J. T. Smith and Thomas P. Barnwell III. Exact reconstruction techniques for tree-structured subband coders. *IEEE Transactions ASSP*, ASSP-34(3):pp. 434:441, June 1986.

[Sim88] Eero Peter Simoncelli. Orthogonal sub-band image transforms. Master's thesis, Massachusetts Institute of Technology, May 1988.

[Vai85] P. P. Vaidyanathan. On power-complementary FIR filters. *IEEE Transactions on Circuits and Systems*, CAS-32(12):pp. 1308–1310, December 1985.

[VD89] P. P. Vaidyanathan and Z. Doganata. The role of lossless systems in modern digital signal processing. *IEEE Transactions Education, Special issue on Circuits on Systems*, 32-3:pp. 181–197, August 1989.

[VG89] M. Vetterli and D. Le Gall. Perfect reconstruction FIR filter banks: some properties and factorizations. *IEEE Transactions ASSP*, 37-7:pp. 1057–1071, July 1989.

[VH88] P. P. Vaidyanathan and P. Q. Hoang. Lattice structures for optimal design and robust implementation of two-band perfect reconstruction QMF banks. *IEEE Transactions ASSP*, ASSP-36-1:pp. 81–94, January 1988.

[VH90] M. Vetterli and C. Herley. Wavelets and filter banks: theory and design. In *Proceedings ICASSP*, pages pp. 1723–1726, Albuquerque, NM, April 1990.

[DP95] "Information-Theoretic Performance of Quadrature Mirror Filters," *IEEE Trans. on Inform. Theory*, vol. 41, pp. 2094–2100, Nov. 1995.

List of Figures

1 A two band quadrature-mirror filter bank 18
2 A qualitative illustration of the mirror symmetry about $\omega = \frac{\pi}{2}$ 19
3 Typical $H_p(\omega)$ 20
4 Typical $F(W)$ 21
5 Typical $F^{'}(W)$ 22
6 Typical $F^{''}(W)$ 23
7 Convex ∩ and Convex ∪ $F^{''}(W)$ 24
8 The two extremes for $F(W)$: The efficient $F(W)$ lies in the middle 25
9 The $P(W)$ for the extremes for $F(W)$ 26
10 $f^{''''}(\omega)$ of Type 1 and Type 2 very close to $f_0^{''''}$ 27
11 $f^{'''}(\omega)$ of Type 1 and Type 2 close to $f_0^{''''}$ 28
12 Changing $f_0(\omega)$ to a $f(\omega)$ of Type 2 29
13 How to find $\omega_{p,max}(9)$ 30
14 Comparison of Johnston's 32 tap "C" filter with the analytical expression: $\omega_p = 1.32 \approx \omega_{p,max}(32) = 1.31$ 31
15 Comparison of the Johnston 32 tap 'C' filter with the 32 tap rectangular window implementation: The window implementation lies between the 32 tap C filter and the theoretical response shown in the previous Figure 32
16 Effects of passband and stop band ripple on $H_p(\omega)$ 33
17 Comparison of the 9 tap implementation with that of Simoncelli and the analytical expression. 34
18 Comparison of the 9 tap implementation with Simoncelli's 9 tap implementation in the log domain (The dotted line represents Simoncelli's design) 35
19 A comparison of the approximately allpass characteristic obtained form Simoncelli's 9 tap filter to that obtained from our 9 tap filter. 36
20 Comparison of the square of the analytical formula with the square of the 9 tap filter characteristic: $\omega_p = 0.895 radians \approx \omega_{p,max}(9) = 0.88 radians$ 37
21 Comparison of the square of the analytical formula with the square of the 16 tap filter characteristic: $\omega_p = 1.05 radians \approx \omega_{p,max}(16) = 1.07 radians$ 38
22 Comparison of the square of the analytical formula with the square of the 32 tap filter characteristic: $\omega_p = 1.32 radians \approx \omega_{p,max}(32) = 1.31 radians$ 39

List of Tables

1 SNR for Increasing Number of Pyramid Stages: 9 tap filters 40
2 Tap values for filters: Starting from the Center tap 41

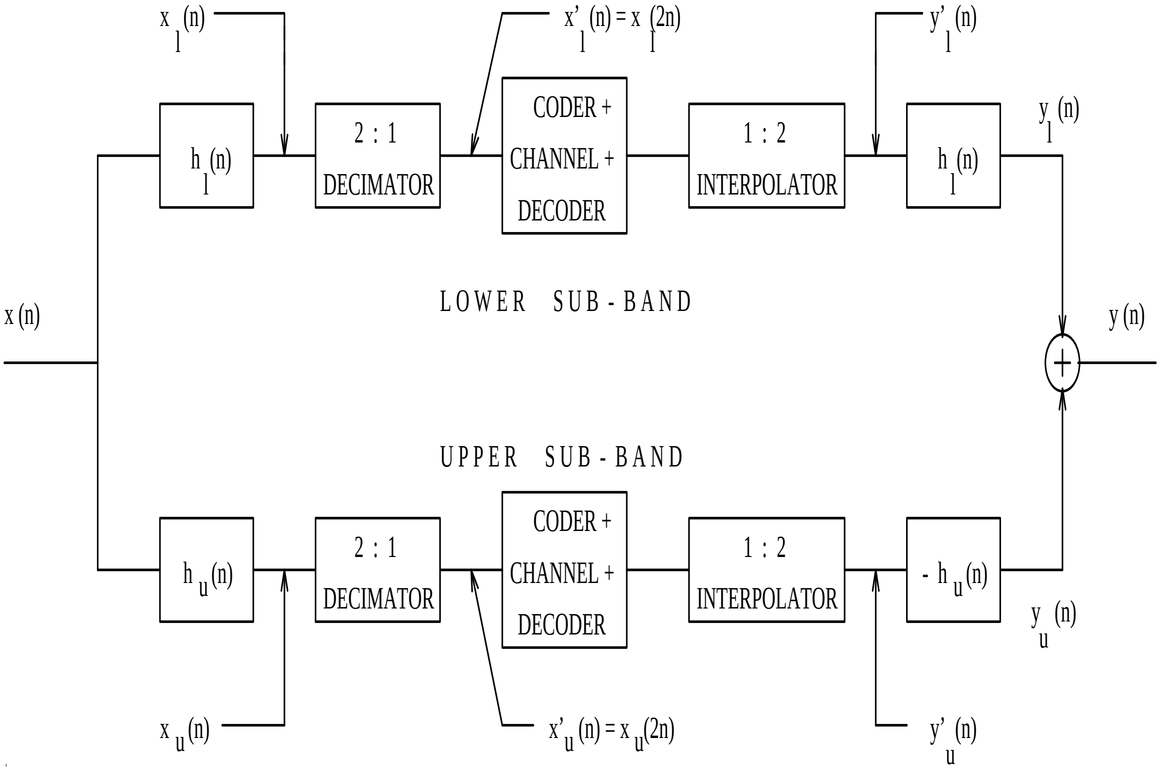

Figure 1: A two band quadrature-mirror filter bank

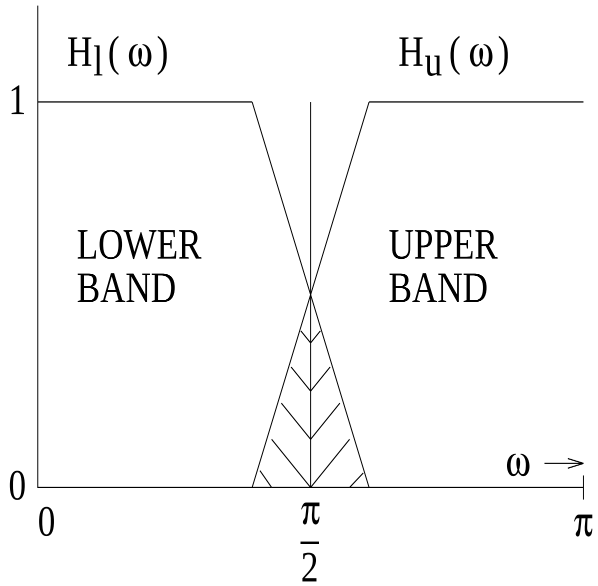

Figure 2: A qualitative illustration of the mirror symmetry about $\omega = \frac{\pi}{2}$

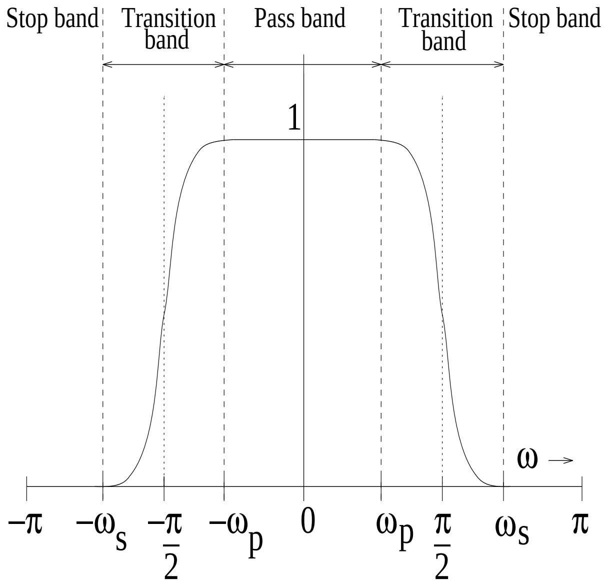

Figure 3: Typical $H_p(\omega)$

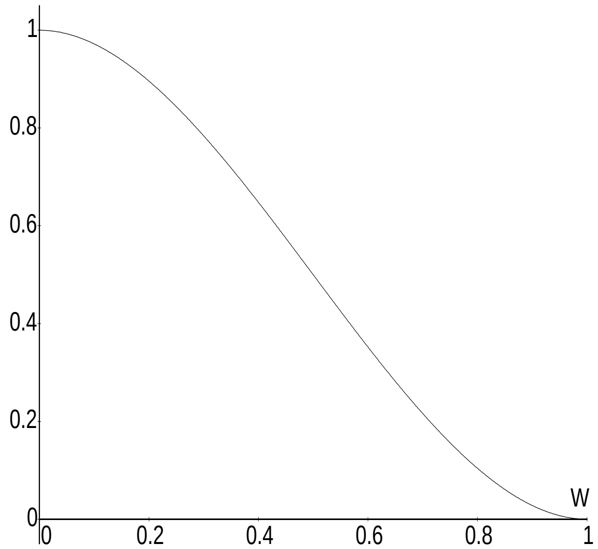

Figure 4: Typical $F(W)$

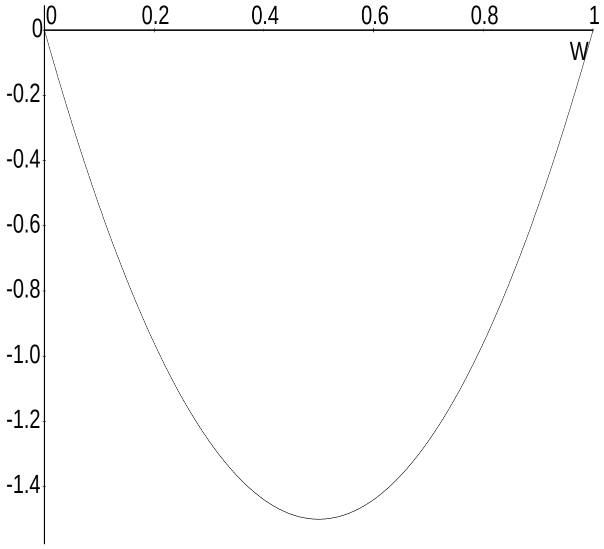

Figure 5: Typical $F'(W)$

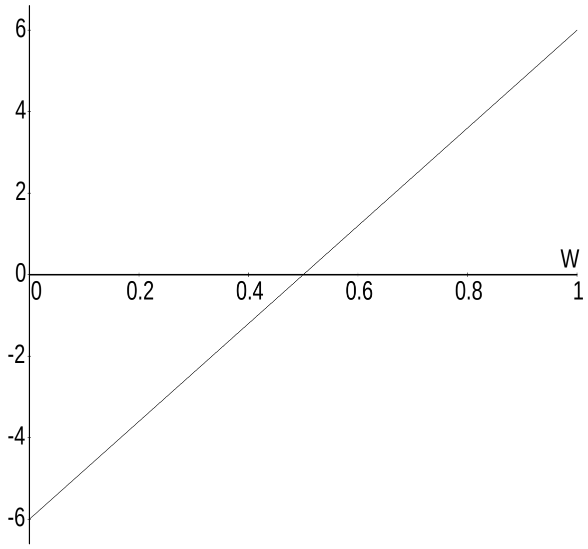

Figure 6: Typical $F''(W)$

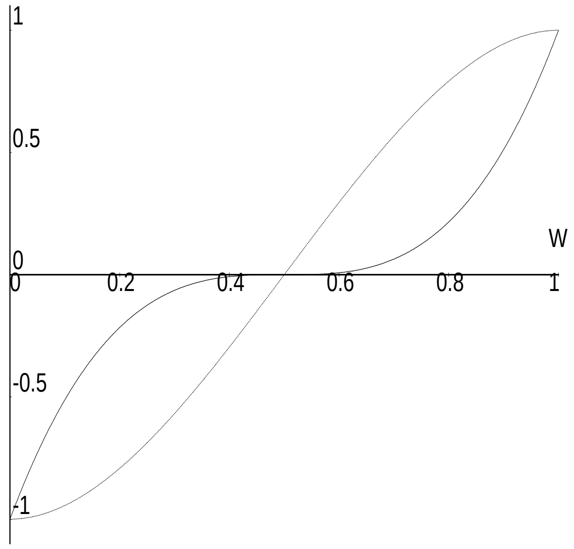

Figure 7: Convex $\cap$ and Convex $\cup$ $F''(W)$

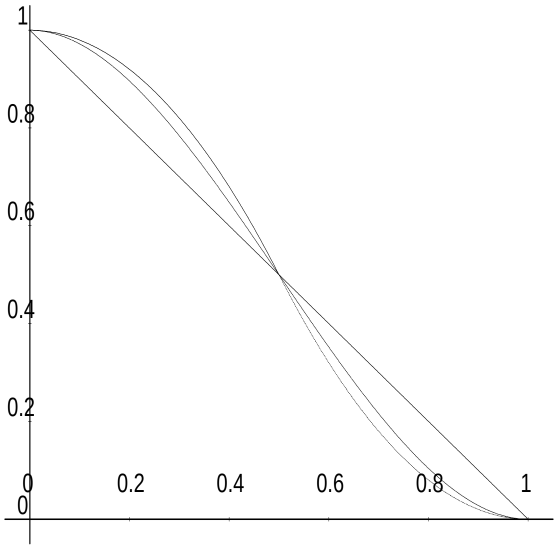

Figure 8: The two extremes for $F(W)$: The efficient $F(W)$ lies in the middle

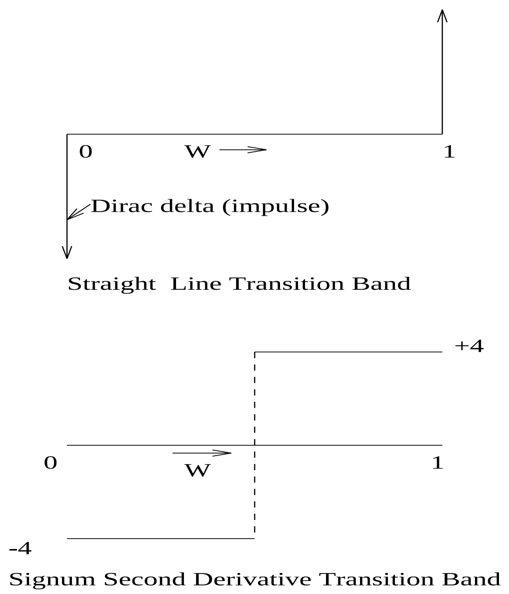

Figure 9: The $P(W)$ for the extremes for $F(W)$

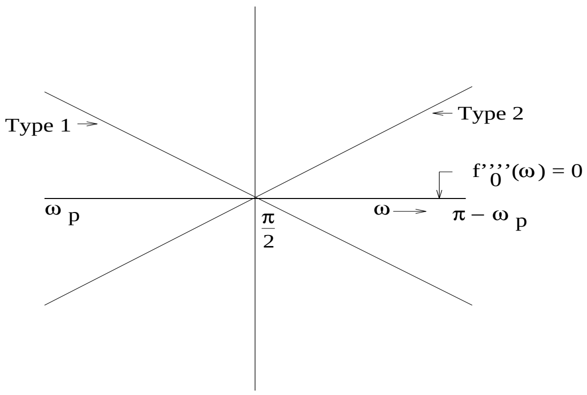

Figure 10: $f''''(\omega)$ of Type 1 and Type 2 very close to f_0''''

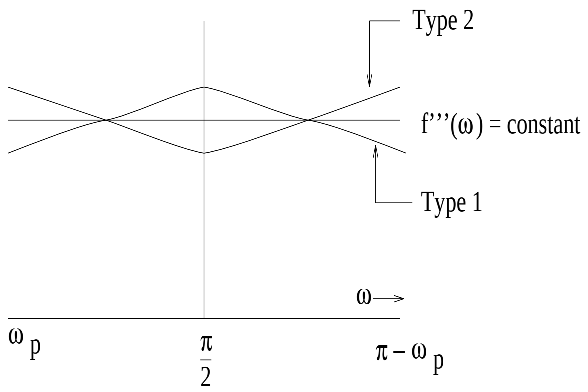

Figure 11: $f'''(\omega)$ of Type 1 and Type 2 close to f_0''''

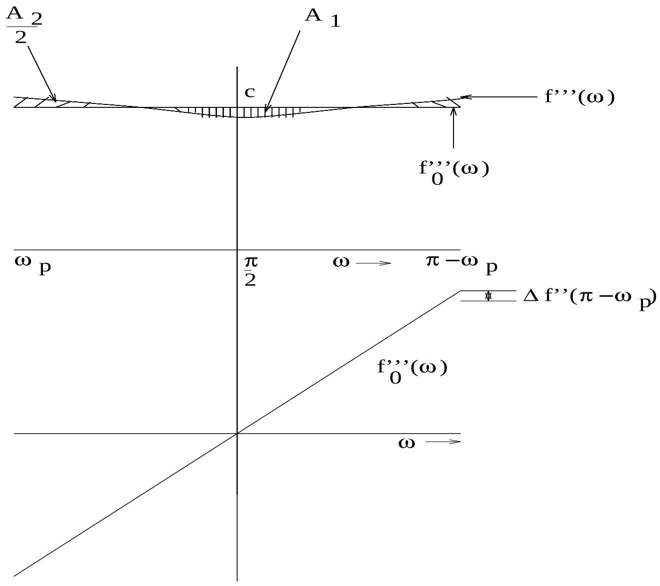

Figure 12: Changing $f_0(\omega)$ to a $f(\omega)$ of Type 2

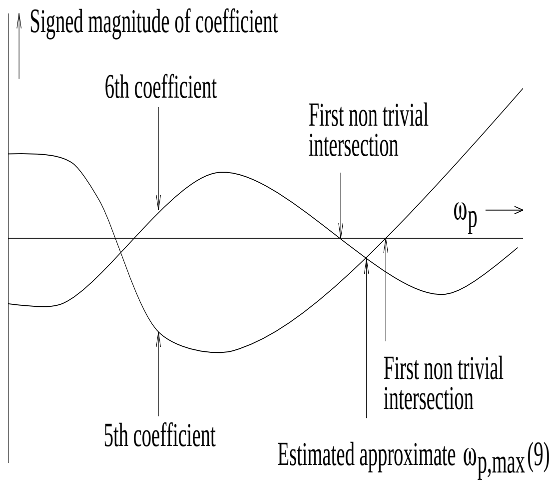

NOT TO SCALE

Figure 13: How to find $\omega_{p,max}(9)$

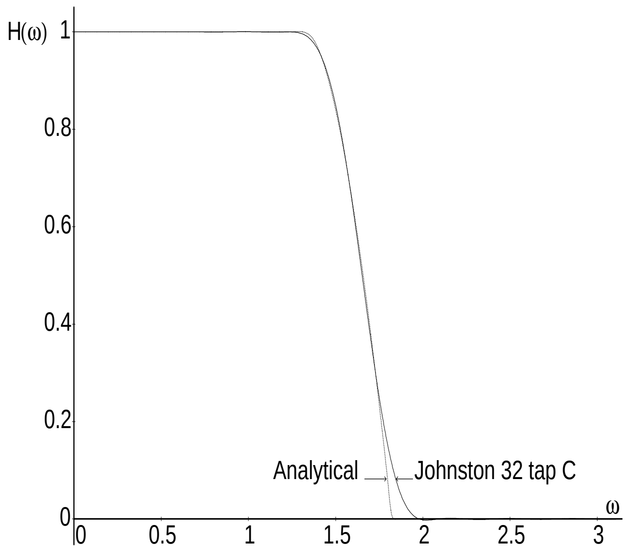

Figure 14: Comparison of Johnston's 32 tap "C" filter with the analytical expression: $\omega_p = 1.32 \approx \omega_{p,max}(32) = 1.31$

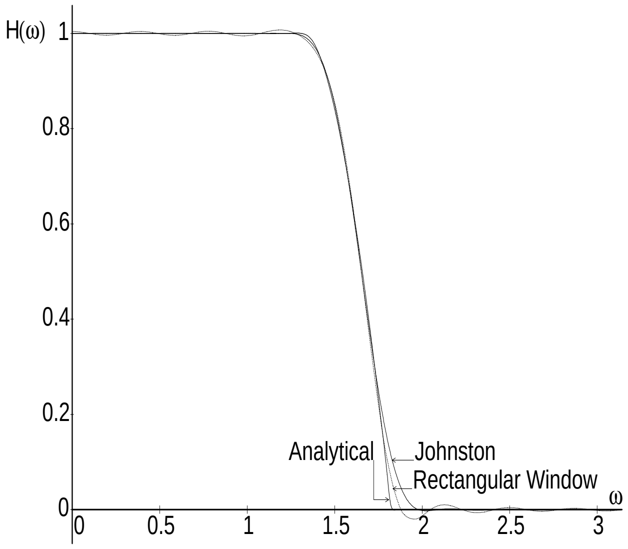

Figure 15: Comparison of the Johnston 32 tap 'C' filter with the 32 tap rectangular window implementation: The window implementation lies between the 32 tap C filter and the theoretical response shown in the previous Figure

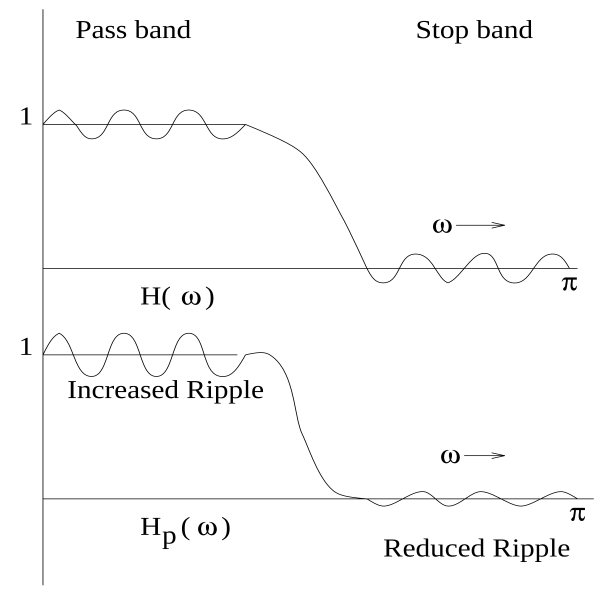

Figure 16: Effects of passband and stop band ripple on $H_p(\omega)$

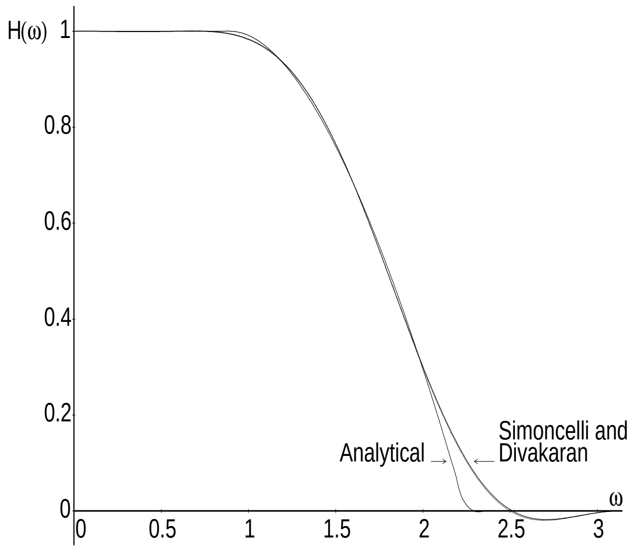

Figure 17: Comparison of the 9 tap implementation with that of Simoncelli and the analytical expression.

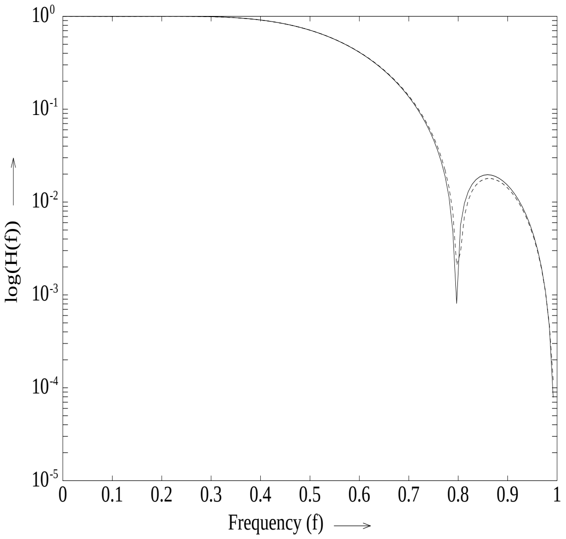

Figure 18: Comparison of the 9 tap implementation with Simoncelli's 9 tap implementation in the log domain (The dotted line represents Simoncelli's design)

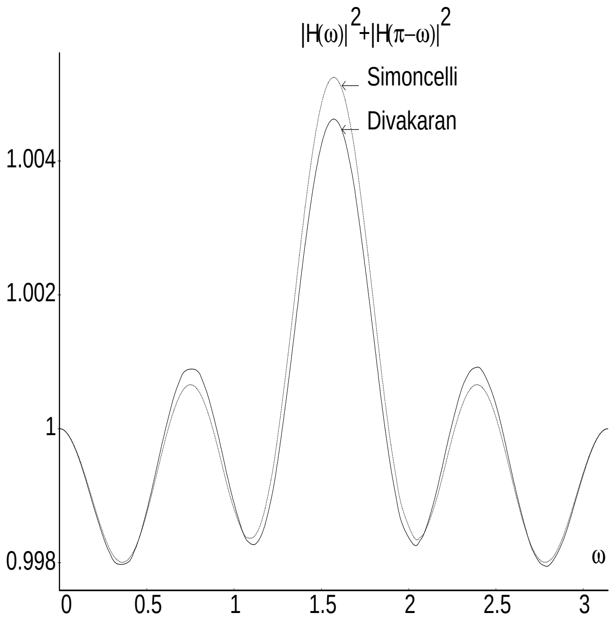

Figure 19: A comparison of the approximately allpass characteristic obtained form Simoncelli's 9 tap filter to that obtained from our 9 tap filter.

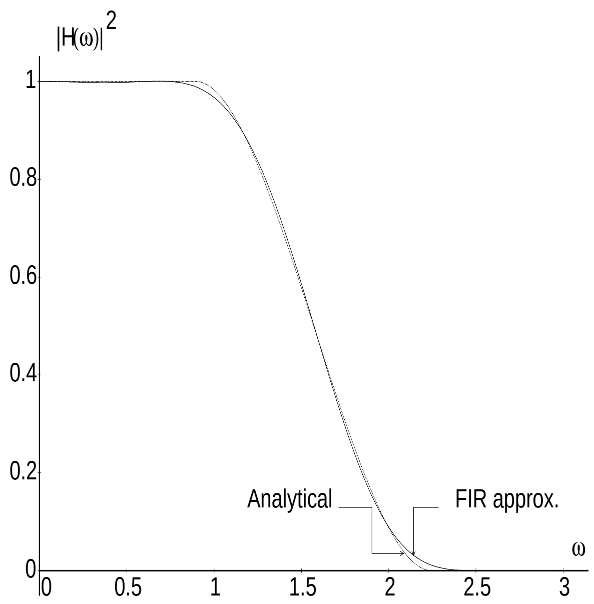

Figure 20: Comparison of the square of the analytical formula with the square of the 9 tap filter characteristic: $\omega_p = 0.895 radians \approx \omega_{p,max}(9) = 0.88 radians$

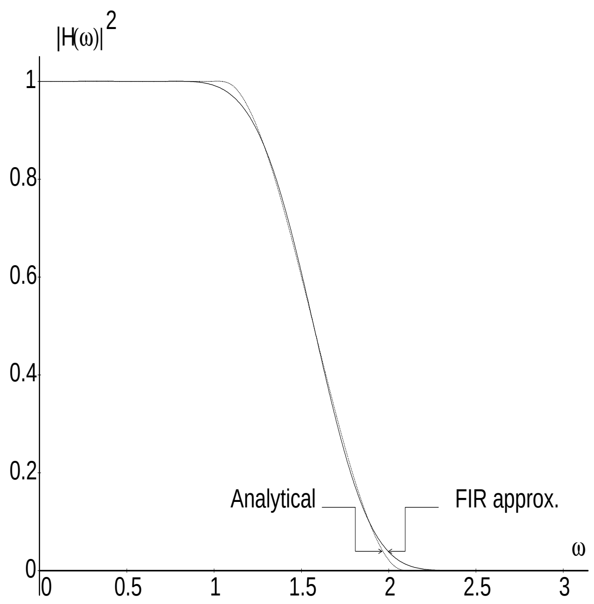

Figure 21: Comparison of the square of the analytical formula with the square of the 16 tap filter characteristic: $\omega_p = 1.05 radians \approx \omega_{p,max}(16) = 1.07 radians$

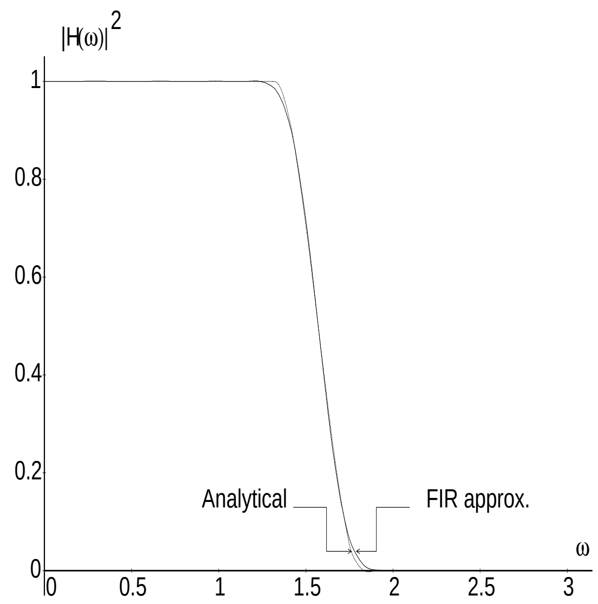

Figure 22: Comparison of the square of the analytical formula with the square of the 32 tap filter characteristic: $\omega_p = 1.32 radians \approx \omega_{p,max}(32) = 1.31 radians$

Table 1: SNR for Increasing Number of Pyramid Stages: 9 tap filters

Image	Pyramid stages	SNR	
		Simoncelli	Divakaran
Lena 256x256	1	∞ dB	∞ dB
	2	73.70 dB	74.09dB
	3	65.80 dB	65.83 dB
Cameraman 256x256	1	90.27 dB	93.28 dB
	2	71.04 dB	71.54 dB
	3	64.95 dB	64.98 dB
Baboon 256x256	1	∞ dB	∞ dB
	2	89.30 dB	96.30 dB
	3	77.20 dB	78.81 dB

Table 2: Tap values for filters: Starting from the Center tap

9 tap	16 tap	32 tap
.56375142	.48062442	.46675062
.29336132	.098407631	.12801628
-.052178906	-.090437812	-.099764009
-.043373601	-.0098975173	-.038721610
.020315472	.027938643	.052570467
	-.00287633240	.014017781
	-.00523493760	-.030636059
	.0014759005	-.0038364670
		.017320018
		-.00027726133
		-.00891695175
		.0013933675
		.0038827994
		-.0012119481
		-.0013145628
		.00072752821